AIChE

An Analysis of Liquid CO_2 Drop Formation with and without Hydrate Formation in Static Mixers

Hideo Tajima
Graduate School of Science and Technology, Niigata University, 2-8050 Ikarashi, Niigata 950-2181, Japan

Ryuichi Nagaosa
Research Institute of Science for Safety and Sustainability, National Institute of Advanced Industrial Science and Technology (AIST), 16-1 Onogawa, Tsukuba, Ibaraki 305-8569, Japan

Akihiro Yamasaki
Dept. of Materials and Life Science, Seikei University, 3-3-1Kichijoji-kitamachi, Musashino, Tokyo 180-8633, Japan

Fumio Kiyono
Institute for Environmental Management Technology, National Institute of Advanced Industrial Science and Technology (AIST), 16-1 Onogawa, Tsukuba, Ibaraki 305-8569, Japan

DOI 10.1002/aic.12167
Published online January 27, 2010 in Wiley Online Library (wileyonlinelibrary.com).

The formation process of CO_2 drops in various types of Kenics Static Mixers was analyzed from the perspective of energy dissipation in the mixer, focusing on the formation of drop surfaces. Experimental studies on CO_2 drop formation were conducted under varying temperatures, pressure, and flow rates, with and without hydrate formation. Analysis of the CO_2 drop size and distribution at several locations within the static mixer was conducted, as of pressure drop in the mixer, to determine dissipation energies. In all the experimental conditions, by considering the surface energy for hydrate formation, the energy required for the formation of CO_2 drops correlated well with total energy dissipation by mixer flow, which is represented by a pressure drop along the mixer. This process has important applications to the formation of liquid CO_2 for ocean disposal as a countermeasure to global warming. © 2010 American Institute of Chemical Engineers *AIChE J,* 56: 2706–2716, 2010
Keywords: drop formation, hydrate, multi-phase flow, static mixer, CO_2 disposal

Introduction

Ocean sequestration of CO_2 at intermediate depths (500–1500 m) has been recognized as a CCS (carbon capture and storage) strategy that might be an effective countermeasure to global warming.[1] In this scenario, CO_2 captured from point sources and liquefied under pressure was piped to the ocean or dispersed from a moving ship.[2] Laboratory-scale experimental studies have demonstrated that upon release the liquid CO_2 phase would break into small drops in seawater[3] because of surface instability.[4] The surface of liquid CO_2 drops would be covered with a thin solid film of clathrate hydrate[5,6] because of pressure and temperature conditions satisfying the thermodynamic requirements for CO_2 hydrate

Correspondence concerning this article should be addressed to A. Yamasaki at akihiro@st.seikei.ac.jp.

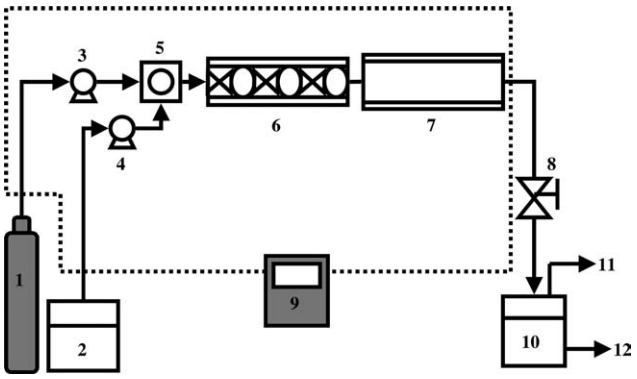

Figure 1. Schematic of the experimental apparatus.

(1) Liquid CO_2 cylinder, (2) water tank, (3) liquid CO_2 supply pump, (4) water supply pump, (5) premerging unit, (6) static mixer unit, (7) postobservation unit, (8) back-pressure controlling valve, (9) cooling unit, (10) hydrate dissociation & vapor–liquid separation unit, (11) CO_2 gas exit, and (12) water exit.

formation.[7] CO_2 hydrate is a solid compound made from hydrogen-bonded water and CO_2 molecules. The formation of CO_2 hydrate is limited to the interface in forming only thin films because the hydrate retards further mass transfer between the liquid CO_2 and water phase.[6] The limited formation of CO_2 hydrate would result in the positive buoyancy of liquid CO_2 drops in the seawater; therefore, the released CO_2 might ascend to the ocean surface.[8] During the ascent, the CO_2 in the drops dissolve into the seawater and might reduce ambient pH, which might in turn disrupt oceanic ecosystems. Environmental impacts caused by the dissolved CO_2, which would be primarily determined by the initial properties of the released CO_2 drops,[9] should be controlled through proper design of the injection process. The optimum size of the liquid CO_2 drops might depend on the storage options. The smaller the drop size, the more severe the environmental impact because of faster CO_2 dissolution to reduce pH. However, an affected area could be limited in this case. For the injection process from a moving ship, smaller drop size is better because dilution of the dissolved CO_2 can be promoted. Proper design of the injection process is important not only from the perspective of controlling environmental impacts[10] but also from that of power consumption. This is because the energy dissipation of oceanic CO_2 injection would affect the power consumption of this CCS strategy. It is essential to minimize power consumption to make CCS a realistic option for counteracting global warming. For example, the formation of smaller drops would in general require larger power consumption.

Tsouris and coworkers have developed a new type of injection system based on the parallel flow of liquid CO_2 and water, and some field experimental results have been reported.[11–17] The present authors have developed another type of injection method for liquid CO_2 drops using Kenics static mixers.[18–20] A two-phase flow of liquid CO_2 and water was introduced to a Kenics static mixer, where the liquid CO_2 phase breaks into drops and disperses in a continuous water phase flow. Laboratory studies demonstrated that use of the Kenics static mixer decreased the average liquid CO_2 drop size, and made the size distribution uniform in comparison to using an empty pipe. This result indicates that the environmental impacts caused by the released CO_2 drops could be controlled more easily, and the fate of the released CO_2 drops is predictable with higher accuracy when the liquid CO_2 is injected through the static mixer.

A drawback to the use of the static mixer is an increase in energy dissipation in the injector. Because of the flow resistance of the mixing elements, the energy dissipation should be higher when static mixers are used compared with an empty pipe. The formation of CO_2 drops would also contribute to energy dissipation because the interface formation requires energy. There are several studies on energy dissipation in static mixers during the drop formation or emulsification in the literature. However, a simple application of previous studies might be insufficient for the two-phase liquid CO_2 and water flow under high-pressure and low-temperature conditions. In addition, our previous study has shown that hydrate formation significantly affects the mixing and formation behaviors of CO_2 drops in the static mixer, although the hydrate formation is limited to a thin film. Therefore, it is necessary to consider the effects of hydrate formation on energy dissipation in the static mixers, which is required for proper design of the injection process. Despite the importance of energy dissipation for the CO_2 injection process, no data are available in the literature for the present system, especially on the effect of hydrate formation.

In this article, energy dissipation during the formation of liquid CO_2 drops in static mixers (Kenics type and its derivatives) was investigated experimentally under various conditions, including those with and without hydrate formation. The contribution of the flow friction of the mixing elements; formation of CO_2 drops; and hydrate formation, were evaluated based on the CO_2 drop size distribution. Based on the results, correlations between the overall energy dissipation and the drop formation energy were obtained. The results provide useful insights on the proper design of a static mixer for CO_2 drop formation in ocean sequestration.

Experimental Section

Flow system

The experimental apparatus used in this study was the same as that used in previous work,[18] and an outline of the system is presented here (Figure 1). The experimental system was composed mainly of three main units: the premerging unit, the static mixer unit, and the postmixing observation unit. The premerging unit is a high-pressure vessel made of stainless steel with a cruciform inner structure. The static mixer unit is composed of a housing pipe with an inner diameter 10.6 mm (Pyrex-glass) and the mixing element (SUS 316). Four types of static mixers were used, equipped with mixing elements of different shapes and configurations. The mixer unit is inserted in the glass housing tube, which itself is inserted into a polycarbonate tube (maximum bearing pressure = 15 MPa). Because both the glass housing tube and the polycarbonate tube are transparent, the behavior of the two-phase flow in the static mixer can be observed directly. Temperature-controlled water was run between the glass housing pipe and the polycarbonate tube to keep the mixer temperature constant. The postmixing

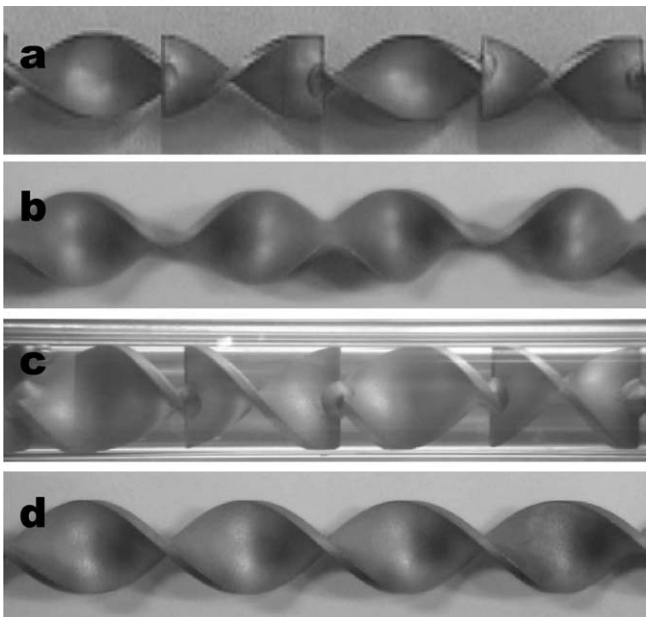

Figure 2. Images of various mixing elements for the static mixer.

(a) Kenics type: KSM, (b) M type: MSM, (c) Right-twist type: RSM, and (d) Spiral type: SSM.

observation unit is made of a Pyrex glass tube with a 10.9 mm inner diameter and 300 mm length, which is connected to the downstream side of the static mixer unit.

Flows of water and liquid CO_2 were introduced separately to the premerging unit, where they underwent preliminarily mixing. The mixed two-phase flow was then introduced to the static mixer unit. The flow velocities of the liquid CO_2 were adjusted from 0.42 to 1.67 cm s^{-1} (reduced volume flow rate, 23.2 and 93.4 cm^3 min^{-1}), and those of water were adjusted from 30.2 to 56.7 cm s^{-1} (reduced volume flow rate, 1.6 and 3.0 dm^3 min^{-1}). The system pressure was controlled to an accuracy of ± 0.01 MPa by a pressure regulator installed downstream of the observation unit. Two pressure and temperature conditions were tested in this study: (1) 7.0 MPa and 277.0 K, which is the region in which CO_2 hydrate is stable, and (2) 7.0 MPa and 285.0 K, under which conditions CO_2 hydrate does not form. Condition (1) simulates ocean pressure and temperature at $\sim$700 m depth. The drop formation process in and release from the mixer were observed directly and recorded by a high-speed video camera (VFC-1000, FOR.A Co.). Size distributions of the CO_2 drops were obtained based on graphical analysis of images of the mixing process (Image J-1.33u, developed by the U.S. National Institute of Health with a Power Macintosh G5 computer). For drop size distribution analysis, images containing at least 700–1000 drops were used.

Static mixers

Four types of static mixers were used, comprised of mixing elements with different shapes and configurations (Figure 2). All mixers were specially designed and supplied by Noritake Co. for the use under high-pressure conditions. All mixing units had the same outer diameter and length. Each comprised 12 identical mixing elements with a length/diameter ratio of 1.5, and an outer diameter of 10.6 mm.

The differences in mixing element shape and configuration resulted in different mixing functions: flow division, flow reversal, and radial mixing. Flow division is the separation of the flow at the front of the mixing element. Radial mixing is where fluids are mixed by radial rotation as fluids pass through the elements. Flow reversal is a mixing process caused by the reversal of flow direction at the connection points between mixing elements.

The Kenics static mixer (Figure 2a) had all three mixing functions. The M-type mixer (MSM) had only radial mixing and flow reversal. The right-twist-type mixer (RSM) had flow division and radial mixing. The spiral-type mixer (SSM) had only the radial mixing function.

Experimental Results and Discussion

Effects of flow rate and hydrate formation on CO_2 drop formation in the Kenics static mixer

In this section, we discuss the size distribution of CO_2 drops formed in the Kenics static mixer. As described earlier, experiments were conducted under two pressure and temperature conditions: (1) 277.0 K and 7.0 MPa (with hydrate), and (2) 285.0 K and 7.0 MPa (without hydrate). Water flow velocities were 30.2 cm s^{-1} (or volume flow rate of 1.6 dm^3 min^{-1}, the lower velocity condition) and 56.7 cm s^{-1} (3.0 dm^3 min^{-1}, the higher velocity condition). The CO_2 flow velocity was fixed at 0.83 cm s^{-1} (volume flow rate

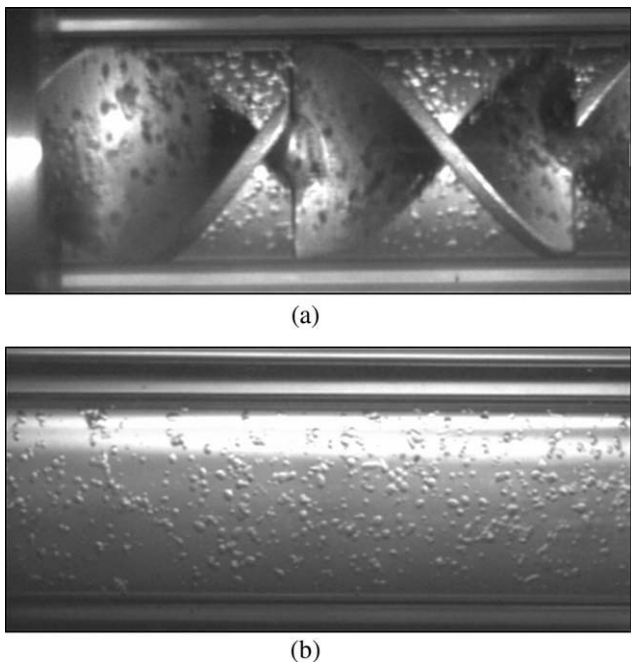

Figure 3. Snapshots of CO_2 drops formed in the static mixer.

(a) In the mixing unit, (b) in the postmixing observation unit.

23.2 cm^3 min^{-1}). The Kenics static mixer used had 24 mixing elements, numbered from the upstream side to the downstream side of the mixer. Snapshots of CO_2 drops observed in the Kenics static mixer and in the postmixing unit are shown in Figure 3. Formation of thin hydrate film was confirmed visually on the CO_2 drop surfaces for condition (1), while no hydrate formation was observed for condition (2) The size distribution of the CO_2 drops in each mixing element was obtained by analyzing the snapshots.

In this article, the Sauter mean diameter (SMD) has been used for the analysis of drop formation. The SMD was used to represent mixing behavior of the liquid CO_2 and water in the static mixer.[21–23] The SMD is defined as

$$\mathrm{SMD} = \frac{\sum N_i D_i^3}{\sum N_i D_i^2} \tag{1}$$

where N_i is the number of CO_2 drops in the ith group having a diameter D_i. The CO_2 drop SMD reduced by mixer diameter D_{SM} observed in each mixing element is shown in Figure 4a. In general, SMD decreased with an increase in the number of mixing elements through which the fluid passed. When the flow rate was 56.7 cm s^{-1}, the reduced SMD decreased quickly at the initial five mixing elements, and became almost constant after the fifth mixing element irrespective of hydrate formation. When the flow rate was 30.2 cm s^{-1}, the reduced SMDs were larger than those for the higher flow rate (56.7 cm s^{-1}) at a given mixing element. For the equal water flow rates, the reduced SMDs were smaller under the hydrate formation condition at a given element. The difference was negligible for the higher water flow rate.

The drop size distribution can be represented by the relative standard deviation (RSD) of the drop diameter.[24] The RSD was calculated according to

$$\mathrm{RSD}^2 = \left(\frac{\sigma}{\mathrm{SMD}}\right)^2 = \frac{\sum_i^N \left(\frac{D_i}{\mathrm{SMD}} - 1\right)^2}{N-1} \tag{2}$$

where N is the total number of the CO_2 drops, and σ is standard deviation of the CO_2 drop size distribution.

The observed CO_2 drop RSDs in each element are shown in Figure 4b.The drop size also decreased with the increasing number of mixing elements. The RSDs of CO_2 drops formed in a given mixing element under the higher flow rate (56.7 cm s^{-1}) were smaller than those under the lower flow rate (30.2 cm s^{-1}). The SMD decreased more quickly with an increasing number of mixing elements in the higher flow velocity (56.7 cm s^{-1}) than in the lower flow velocity (30.2 cm s^{-1}). The RSDs where hydrate formed were smaller than those without hydrate formation. The RSD of the CO_2 drops decreased up to the initial five mixing elements and was almost unchanged after that. The decreasing trends of SMD and RSD in the mixer were consistent with previous research on liquid drop formation in static mixers.[18,25,26]

Size distributions (drop volume-based) of CO_2 drops observed at the fifth mixing element are shown for cases with hydrate formation (Figure 5) and without hydrate formation (Figure 6). Where there was hydrate formation, a Gaussian-like distribution was observed for both flow velocity conditions, but the peak location shifted to smaller sizes and the distribution became narrower by increasing flow velocity. Where there was no hydrate formation, a bimodal size distribution was observed for the lower flow velocity (30.2 cm s^{-1}), while a narrow Gaussian-like distribution was observed for the case with the higher water velocity (56.7 cm s^{-1}). In addition, the distribution peak shifted to smaller sizes with increasing flow velocity.

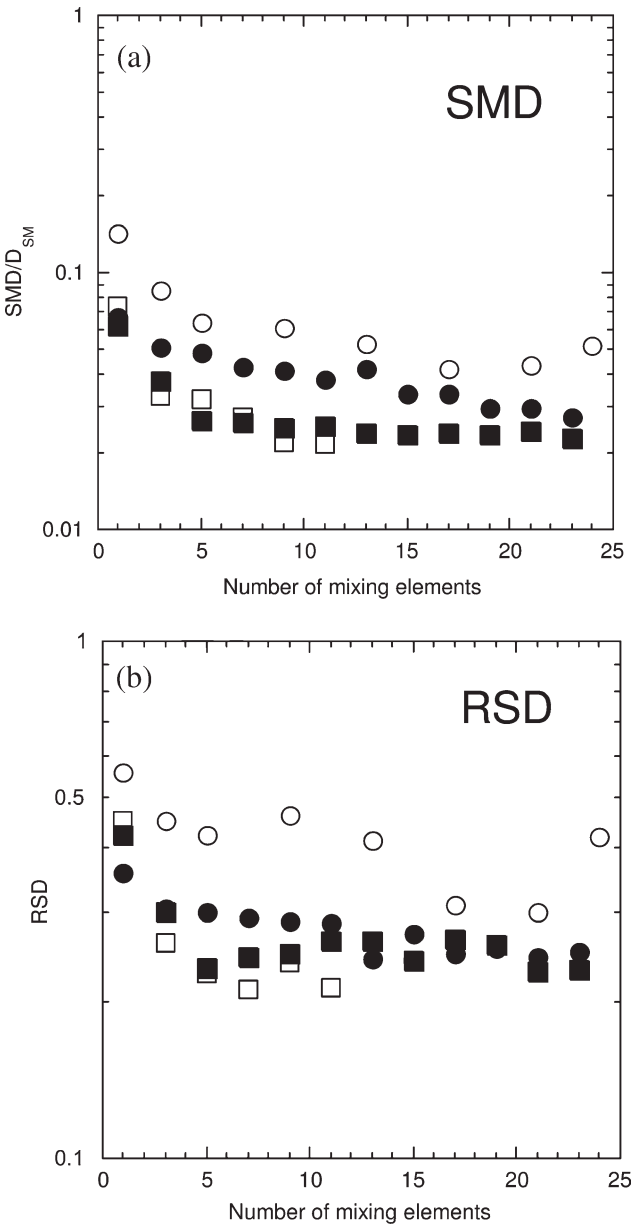

Figure 4. Variations of (a) SMD/D_{SM} and (b) RSD with the number of mixing elements.

Conditions: pressure 7.0 MPa, CO_2 flow rate = 0.83 cm s^{-1} (23.2 cm^3 min^{-1}). Key: ●: 278.0 K (with hydrate), water flow rate = 30.2 cm s^{-1} (1.6 dm^3 min^{-1}), CO_2 volume fraction = 0.008. ■: 278.0 K (with hydrate), water flow rate = 56.7 cm s^{-1} (3.0 dm^3 min^{-1}), CO_2 volume fraction = 0.015. ○: 285.0 K (without hydrate), water flow rate = 30.2 cm s^{-1} (1.6 dm^3 min^{-1}) CO_2 volume fraction = 0.008. □: 285.0 K (without hydrate), water flow rate = 56.7 cm s^{-1} (3.0 dm^3 min^{-1}), CO_2 volume fraction = 0.015.

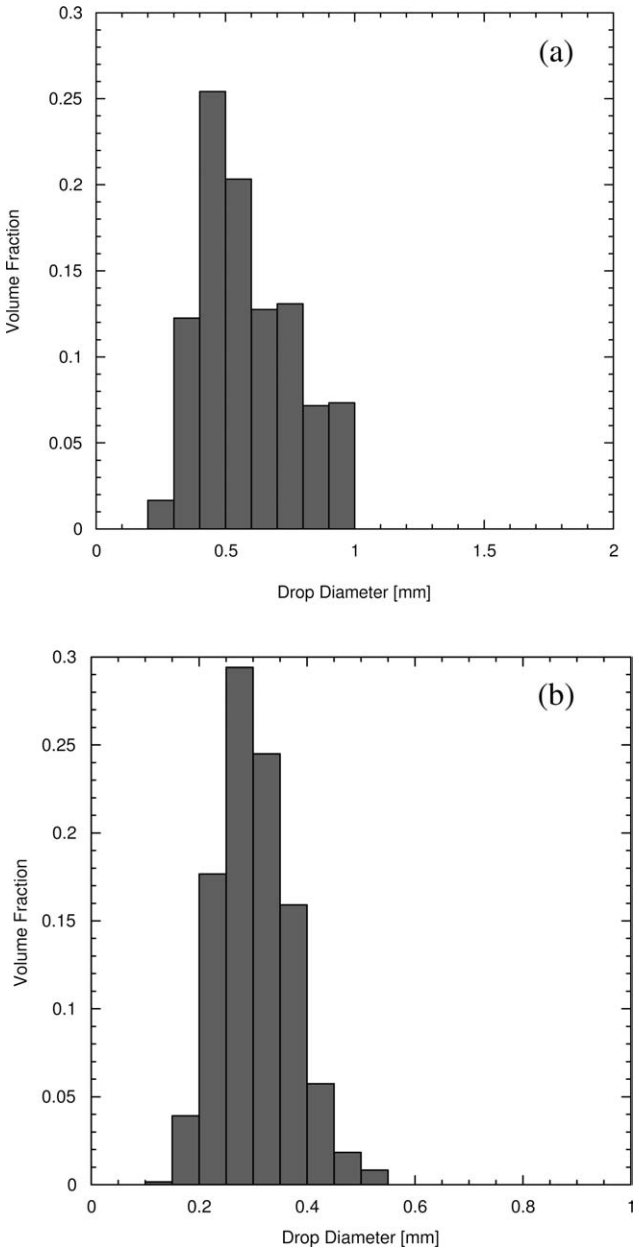

Figure 5. Size distributions of the liquid CO_2 drops observed at the fifth mixing elements with hydrate formation (278.0 K and 7.0 MPa).

(a) Water flow rate = 30.2 cm s^{-1} (1.6 dm^3 min^{-1}), CO_2 volume fraction = 0.008 and (b) water flow rate = 56.7 cm s^{-1} (3.0 dm^3 min^{-1}), CO_2 volume fraction = 0.015.

For the higher water velocity (56.7 cm s^{-1}), both SMD and RSD decreased quickly at the initial five mixing elements, after which they were almost constant. The size distribution is narrow and Gaussian-like at the fifth element. This indicates that drop formation is stabilized after the fifth element where water velocity is higher, irrespective of hydrate formation. The drop size distribution in a static mixer is the result of drop breakup and coalescence. The increasing flow velocity would increase the both rates of breakup and coalescence. However, the rate increase of breakup was faster than that of coalescence. Thus, by increasing the velocity, i.e., increasing the energy input, the breakup rate exceeded the coalescence rate and consequently the peak size of drops shifts to smaller ranges. When the flow velocity is decreased, the breakup rate decreases faster than the coalescence rate, and the drop size distribution shifts to larger drop sizes.

The bimodal size distribution shown in Figure 6a indicates that the breakup rate is not sufficiently high under the lower

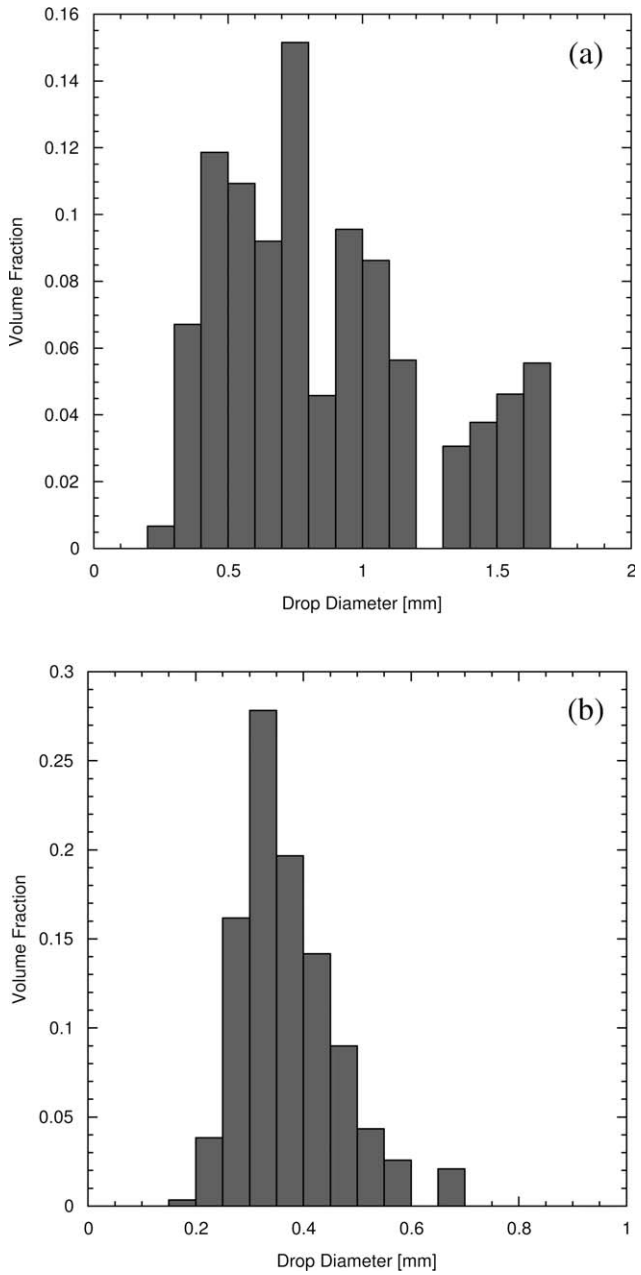

Figure 6. Size distributions of the liquid CO_2 drops observed at the fifth mixing elements without hydrate formation (285.0 K, 7.0 MPa).

(a) Water flow rate = 30.2 cm s^{-1} (1.6 dm^3 min^{-1}), CO_2 volume fraction = 0.008 and (b) water flow rate = 56.7 cm s^{-1} (3.0 dm^3 min^{-1}), CO_2 volume fraction = 0.015.

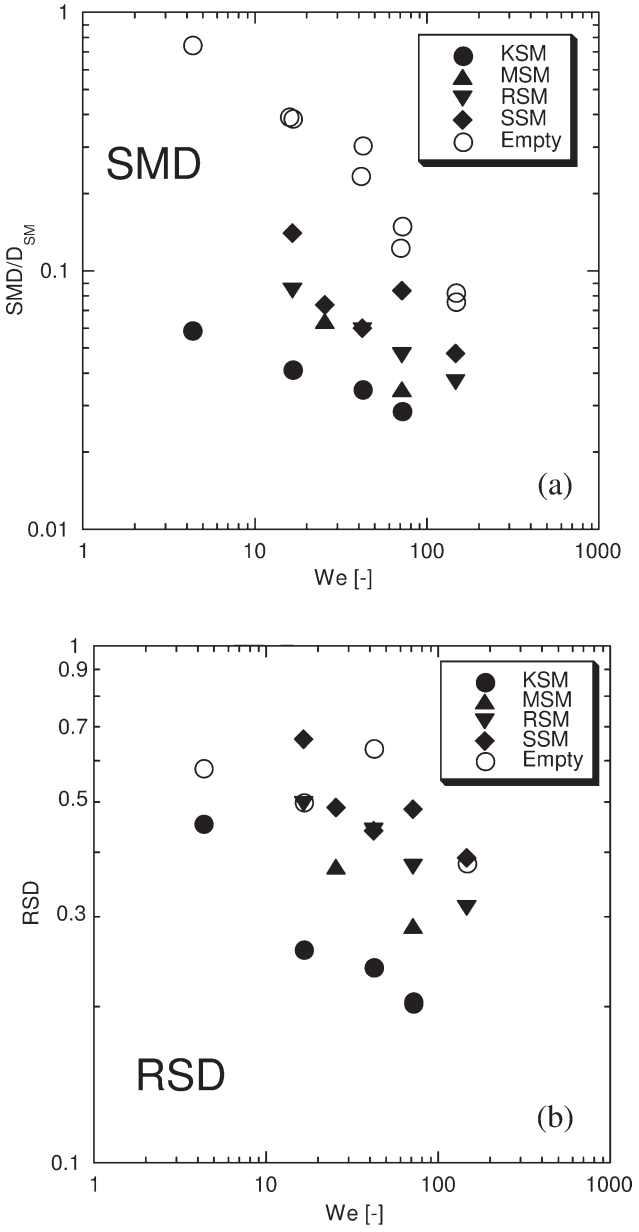

Figure 7. Relationship between the reduced Sauter Mean Diameter (SMD) and Weber number (We), and between Relative Standard Deviation (RSD) and Weber number of the diameter of CO_2 drops for various types of static mixers.

Conditions: Temperature = 277.0 K; Pressure = 7.0 MPa (with hydrate formation); water flow velocity = 37.7 cm s^{-1} (2.0 dm^3 min^{-1}): CO_2 volume fraction = 0.012.

flow velocity. The drop size before introduction to the static mixer is distributed broadly in the range of 2–8 mm (results not shown). Thus, the larger drops would correspond to the remaining drops formed before injection into to the mixer. The bimodal size distribution was observed only for the condition without hydrate formation, which suggests that the breakup of the drops will be promoted by the hydrate film on the surface.

In this study, the volume fraction of the dispersed phase (CO_2) was adjusted in the range 0.008–0.015. Previous studies of drop formation from liquid–liquid in static mixers showed that drop size is not affected by the volume fraction of the dispersed phase provided that the volume fraction is smaller than 0.3.[27,28] The present results for conditions with the higher water velocity (56.7 cm s^{-1}) are consistent with published results in the literature. The effect of the volume fraction of the dispersed phase will be examined and reported in future work.

Effect of mixing element type on CO_2 drop formation

In this section, the effect of mixing element shape and configuration on CO_2 drop formation is examined by comparing the four types of static mixer (KSM, MSM, RSM, and SSM). All the mixers have 24 mixing elements. For comparison, an empty pipe with the same volume was also used. Experiments were conducted under condition (1) as in the previous section (277.0 K, 7.0 MPa) where the CO_2 hydrate phase is stable. The water flow velocity was adjusted from 30.2 to 56.7 cm s^{-1}, while the CO_2 flow velocity was fixed.

Figure 7 shows the reduced SMD/D_{SM} of the CO_2 drops observed at the end of the different static mixers, as a function of Weber number. The Weber number is defined as

$$\mathrm{We} = \frac{\rho u^2 D_{\mathrm{SM}}}{\sigma_s} \tag{3}$$

where ρ is the density of the water phase, u is the flow velocity of the water phase, and σ_s is the water-side surface tension. Data sourced from the literature were used for the interfacial tension (21.5 mN m^{-1}) of the CO_2-hydrate-water system.[29] The SMD/D_{SM} correlated well with the Weber number for each mixer; the SMD decreased with increasing Weber number, or equivalently the water flow velocity. It is known that the SMD/D_{SM} of the drops formed in Kenics static mixers from liquid–liquid flows are well correlated with the Weber number.[21,23] In our previous work, we demonstrated that the relationship could be applied in a liquid CO_2-water system with hydrate formation,[18,20] and the correlation equation is

$$\frac{\mathrm{SMD}}{D_{\mathrm{SM}}} = \alpha \times \mathrm{We}^{-\beta} \tag{4}$$

It is confirmed in this article that the correlation is valid for each type of static mixer.

For the same Weber number, the CO_2 drop SMD increased in the order KSM < MSM < RSM < SSM < Empty pipe. As the dependency of the SMD on the Weber number was the same as this order, the difference in the SMD between static mixers decreased with increasing Weber number. The RSD of the drops are plotted against Weber number in Figure 7. The RSD of the CO_2 drops formed with KSM was the smallest, and increased in the order MSM < RSM < SSM < Empty pipe, which is the same as the SMD order.

Figure 8 shows the size distributions of the CO_2 drops with hydrate, observed at the postmixing observation unit in various static mixers. As expected from the RSD, the narrowest liquid CO_2 distribution was observed when the KSM

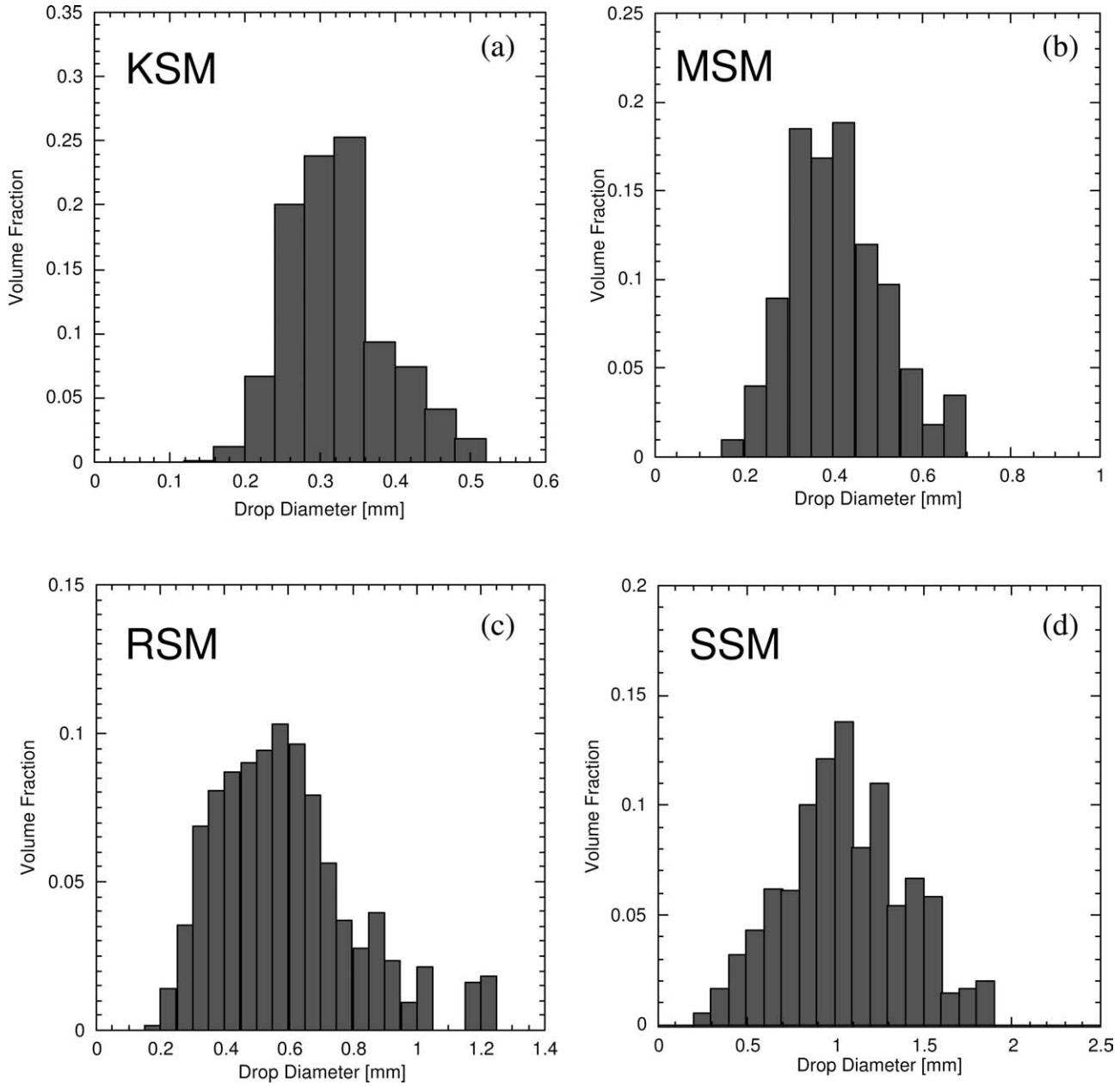

Figure 8. Size distributions of CO_2 drops observed at the fifth mixing elements for various types of static mixers.

Conditions: Temperature = 277.0 K; Pressure = 7.0 MPa (with hydrate formation); water flow velocity = 37.7 cm s^{-1} (2.0 dm^3 min^{-1}); CO_2 volume fraction = 0.012. (a) KSM; SMD = 0.313 mm: RSD = 0.205, (b) MSM; SMD = 0.379 mm: RSD = 0.287, (c) RSM; SMD = 0.514 mm: RSD = 0.374, and (d) SSM; SMD = 0.923 mm: RSD = 0.483.

was used, and the distribution width increased in the same order of RSD, KSM < MSM < RSM < SSM.

The aforementioned results can be explained in terms of the mixing functions of each static mixers type. The KSM has all three mixing functions (flow division, flow reversal, and radial mixing) which would result in the smallest SMD and the narrowest distribution of CO_2 drops. Conversely the SSM, which has only the radial mixing function, shows the largest SMD and the widest size distribution (aside from the empty pipe) and may have no special mixing function. By comparing the results between the RSM and MSM, the flow reversal function has a more significant effect on the size reduction of the CO_2 drops with a narrower size distribution than the flow division function.

The relationship between CO_2 drop surface energy and total energy dissipation in static mixers

The size distributions of CO_2 drops can be used for analyzing energy dissipation in the static mixers. The rate of energy dissipation in a static mixer, E, is dependent on the drop in pressure (ΔP_{SM}),[21–23,27] that is,

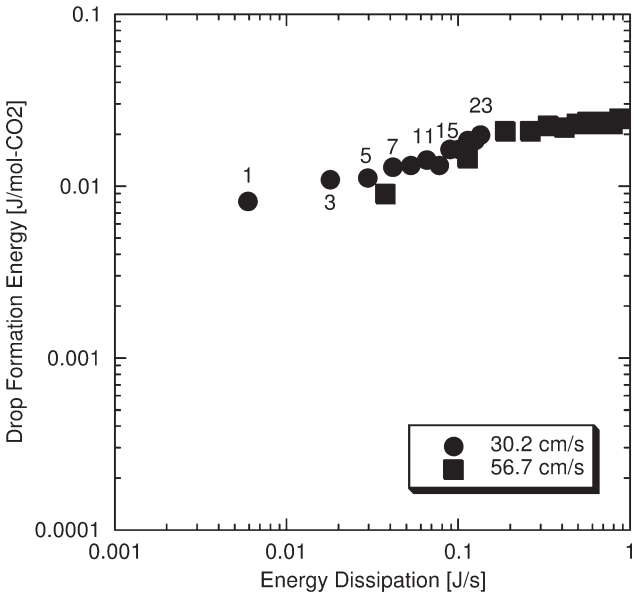

Figure 9. Correlation between energy dissipation for drop formation and overall energy dissipation in the Kenics static mixer with hydrate formation.

Temperature = 277.0 K; Pressure = 7.0 MPa (with hydrate formation); water flow velocity = 37.7 cm s^{-1} (2.0 dm^3 min^{-1}, CO_2 volume fraction = 0.012) and 56.7 cm s^{-1} (3.0 dm^3 min^{-1}, CO_2 volume fraction = 0.015). The number indicates the number of the mixing element.

$$E = u\frac{\Delta P_{SM}}{\rho L_{SM}} \tag{5}$$

where ρ is the fluid density, u is the fluid flow velocity, and L_{SM} is the length of the static mixer. The pressure drop can be expressed as a function of the friction coefficient of the static mixer (f_{SM}) and the number of the mixing elements in the static mixer (N_E), according to the Fanning equation[23,30,31];

$$\Delta P_{SM} = 4f_{SM}\left(\frac{\rho u^2}{2}\right)\left(\frac{L_{SM}}{D_{SM}}\right) = 3f_{SM}\rho u^2 N_E, \tag{6}$$

where D_{SM} is the diameter of the static mixer. Note the relationship $L_{SM} = 1.5D_{SM}N_E$ holds for all mixers used in this study. The friction coefficient of each mixer was determined experimentally by measuring the pressure drop with pure water flow as function of the Reynolds number, Re, because no literature data are available for the friction coefficients of MSM, RSM, and SSM. For the same Re, the friction coefficient, f_{SM}, was found to increase in the order SSM < RSM < MSM < KSM, which is opposite to the CO_2 drop SMD and RSD. In other words, the energy dissipation in the static mixer also increases in this order.

On the basis of the friction coefficients, the energy dissipation rate in each mixer was estimated from Eqs. 5 and 6. It was assumed that the flow velocity and the density of the fluid in the static mixer were equal to those of the water flow, which can be rationalized by the negligible fraction of liquid CO_2 in the total flow rate. The maximum value of the volume fraction was 0.06.

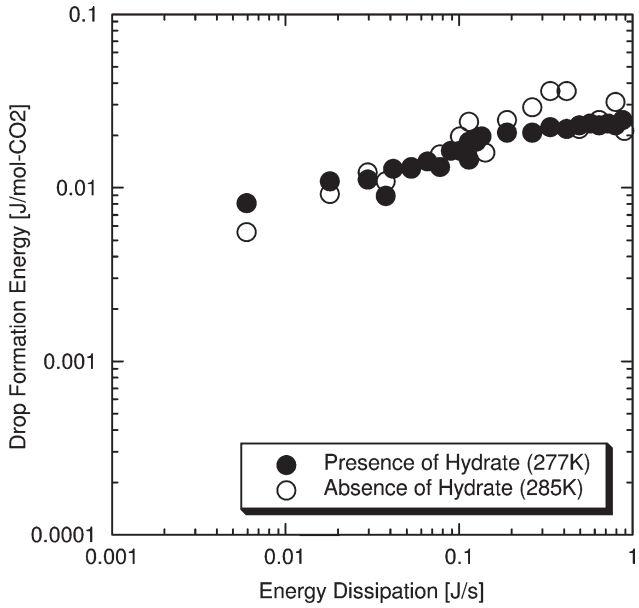

Figure 10. Correlation between energy dissipation for drop formation and the overall energy dissipation in the Kenics static mixer with and without hydrate formation.

Conditions: Water flow velocity = 37.7 cm s^{-1} (2.0 dm^3 min^{-1}, CO_2 volume fraction = 0.012.) and 56.7 cm s^{-1} (3.0 dm^3 min^{-1}, CO_2 volume fraction = 0.015). Keys: ● With hydrate formation: temperature = 277.0 K, pressure = 7.0 MPa. ○ Without hydrate formation: temperature = 285.0 K, pressure = 7.0 MPa.

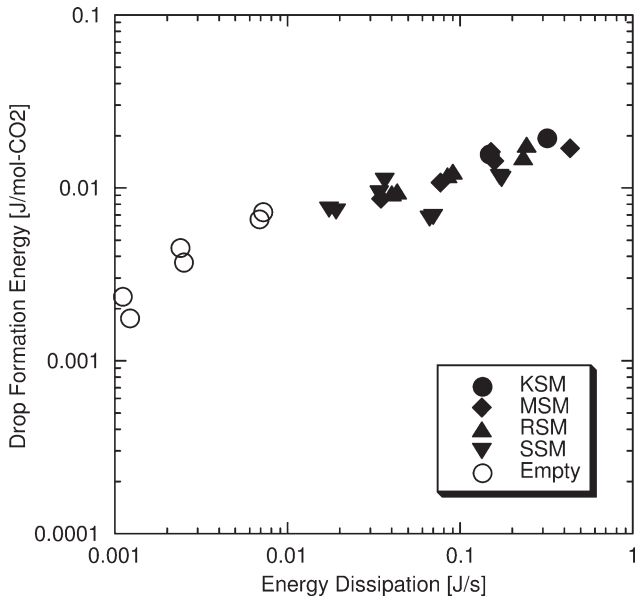

Figure 11. Correlation between energy dissipation for drop formation and overall energy dissipation for various types of static mixers and empty pipe with hydrate formation.

Different keys represent different types of static mixers (Figure 2). Conditions: Temperature = 277.0 K; pressure = 7.0 MPa; water flow velocity = 30.2–56.7 cm s^{-1}; CO_2 flow velocity = 0.42–1.67 cm s^{-1}.

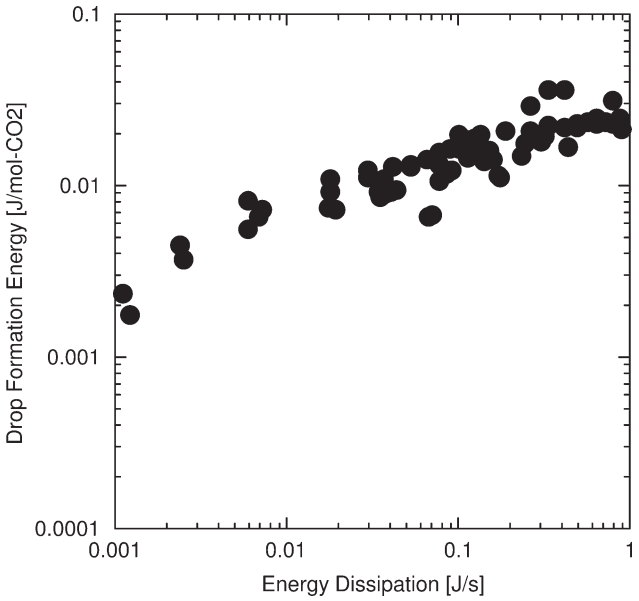

Figure 12. Correlation between energy dissipation for drop formation and overall energy dissipation for various types of static mixers and empty pipe with and without hydrate formation.

Conditions: Temperature = 277.0 K (with hydrate) and 285.0 K (without hydrate); pressure = 7.0 MPa; water flow velocity = 30.2–56.7 cm s^{-1}; CO_2 flow velocity = 0.42–1.67 cm s^{-1}.

The energy required for the formation of CO_2 drops can be estimated from the energy required for the surface extension. The energy, E_s, can be expressed by

$$E_s = \int_0^\infty [N_f(D)\pi\sigma_f D^2 - N_i(D)\pi\sigma_i D^2]dD \tag{7}$$

where D is the drop diameter, $N_i(D)$ and $N_f(D)$ are the number distribution of the CO_2 diameter at the initial and final stage, respectively. σ_i and σ_f are the interfacial tensions of liquid CO_2—water at the initial and final stage, respectively. π is the circle ratio. In this case, the initial number of CO_2 drops before the static mixer is much smaller after, and the overall energy for the CO_2 drop formation can be approximated by

$$E_s \approx \int_0^\infty N_f(D)\pi\sigma_f D^2 dD \tag{8}$$

Figure 9 shows the relationship between the energy dissipation calculated from the pressure drop, and the energy required for formation of CO_2 drops with the hydrate in the Kenics static mixer (277 K and 7.0 MPa). A good correlation was observed between energy dissipation and drop formation energy, irrespective of the number of mixing elements or the water flow rates. The slope of the log–log plots in Figure 9 is ~0.3. This indicates that the ratio of the energy dissipation for the liquid CO_2 formation to the total energy dissipation in the mixer became smaller, either with increasing the number of mixing elements through which the fluid passed or increasing the flow rates. Therefore, energy dissipation for processes other than drop formation would increase with increasing the number of the elements or the flow rate. The result for CO_2 drops covered with hydrate is, although "solid" CO_2 hydrate is involved in the present system, is similar to other results published in the literature for liquid–liquid systems.[22,30,32,33]

Figure 10 shows the relationship between the energy dissipation in the Kenics static mixer and the drop formation energy. A common correlation could be observed irrespective of the hydrate formation.

Figure 11 shows the relationship between the drop formation energy and the energy dissipation in the various types of static mixers and the empty pipe. A correlation was observed between the drop formation energy and the energy dissipation in the mixer. However, a discrepancy in the slope was observed between the results from the empty pipe and those from the static mixers. The results suggest that a larger energy would be required for the formation of smaller drops in the static mixers, compared with the formation of larger drops in the empty pipe. However, when the smaller drops are formed the higher portion of the energy would be dissipated in the static mixer due to the fluid-wall friction.

All the results are plotted in Figure 12. It can be seen that a good correlation exists between the overall drop formation energy and the energy dissipation in the static mixer,

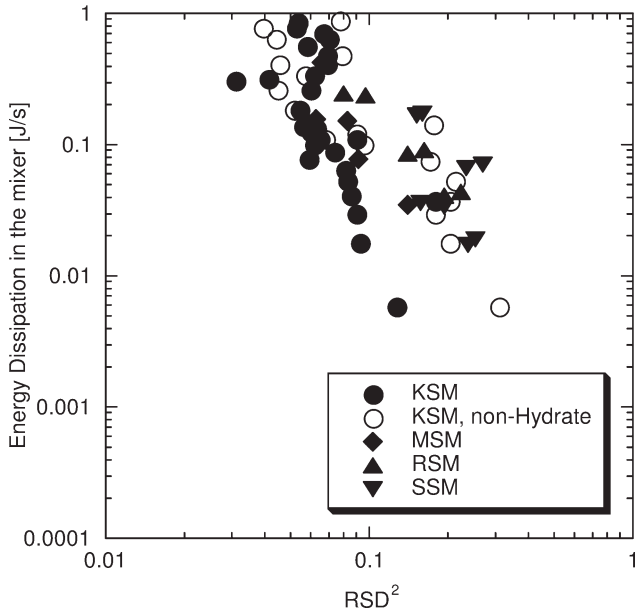

Figure 13. Correlation between overall energy dissipation for various types of static mixers and RSD of drop diameter with (open symbols) and without hydrate formation (closed symbols).

Different symbols represent different static mixer types (Figure 2). Conditions: Temperature = 277.0 K (with hydrate) and 285.0 K (without hydrate); pressure = 7.0 MPa; water flow velocity = 30.2–56.7 cm s^{-1}; CO_2 flow velocity = 0.42–1.67 cm s^{-1}.

irrespective of water flow velocity, shape and number of mixing elements, and formation of hydrate on the drop surface.

Energy dissipation in the static mixer and local drop formation energy

The RSD^2 implies the distribution of the formation energy of individual drops, and is assumed to be the distribution of local drop formation energy at the microscale in the fluid.

The RSD and the shape of the drop size distribution are affected greatly by the shape of the mixing element. The narrow size distribution shows that the drop formation energy is spread widely through the fluid in the static mixer. The shape of the mixing element, *i.e.*, the mixing function of the static mixer, plays a role in the distribution of local drop formation energy in the fluid.

Figure 13 shows the relationship between RSD^2 and the energy dissipation in the static mixer. The KSM consumes lower energy for a certain distribution than the other mixers. The results for the other mixers imply that the energy is not effectively used for drop formation, and the distribution of the local drop formation energy in the fluid is very wide. Extra energy must be added to the fluid for drop formation. Because of its mixing element shape, the KSM is a most suitable for achieving optimal distribution of local drop formation energy.

Conclusions

The following conclusions could be drawn from this study.

1 The size of the CO_2 drops formed in the Kenics static mixer decrease more rapidly by increasing the number of mixing elements at a higher flow rate.

2 The formation of CO_2 hydrate on the drop surface reduced drop size, and narrowed the size distribution. However, these effects were not significant when the flow velocity was high (56.7 cm s^{-1}, 3.0 dm^3 min^{-1}).

3 All the three mixing function of the Kenics static mixers (flow division, flow reversal, and radial mixing) affect the size and distribution of CO_2 drops. However, the flow reversal function plays the most significant role in reducing drop size and in narrowing the size distribution.

4 A good correlation was observed between the energy for drop formation (surface energy) and the energy dissipation in the static mixer (friction), irrespective of the flow rate, hydrate formation, or type of static mixer. A higher proportion of energy will be consumed/dissipated for the formation of smaller drops.

Literature Cited

1. Herzog HG, Drake EM, Adams EE. *CO_2 Capture, Reuse, and Storage Technologies for Mitigating Global Climate Change—A White Paper*. Cambridge, MA: Massachusetts Institute of Technology. 1997; DOE Order No. E-AF22–96PC01257. http://sequestration.mit.edu/pdf/WhitePaper.pdf.
2. Ozaki M. CO_2 injection and dispersion in mid-ocean by moving ship. *Waste Manag*. 1997;17:369–373.
3. Masutani SM, Kinoshita CM, Nihous GC, Ho T, Vega LA. An experiment to simulate ocean disposal of carbon dioxide. *Energy Convers Manag*. 1993;34:865–872.
4. Teng H, Yamasaki A, Shindo Y. Effect of hydrates on instability of liquid CO_2 jet in the deep ocean. *Energy*. 1997;22:273–278.
5. Brewer PG, Friederich GE, Peltzer ET, Orr FM Jr. Direct experiments on the ocean disposal of fossil fuel CO_2. *Science*. 1999;284:943–945.
6. Sakai H, Gamo T, Kim ES, Trutsumi M, Tanaka T, Ishibashi J, Wakita H, Yamamoto M, Oomori T. Venting of carbon dioxide-rich fluid and hydrate formation in the mid-Okinawa trough Backarc basin. *Science*. 1990;248:1093.
7. Song KY, Kobayashi R. Water content of CO_2 in equilibrium with liquid water and/or hydrates. *SPE Formation Evaluation*. December 1997; 500.
8. Brewer PG, Peltzer ET, Friederich G, Rehder G. Experimental determination of the fate of rising CO_2 droplets in seawater. *Environ Sci Technol*. 2002;36:5441–5446.
9. Liro CR, Adams EE, Herzog HJ. Modeling the release of CO_2 in the deep ocean. *Energy Convers Manag*. 1992;33:667–674.
10. Sato T, Hama T. Numerical simulation of dilution process in CO_2 ocean sequestration. In: Proceedings of the 5th International Conference on Greenhouse Gas Control Technologies. Collingwood, Australia: CSIRO, 2001:475–480.
11. West OR, Tsouris C, Liang L, Lee SY, McCallum SD. Negatively bouyant CO_2-hydrate composite for ocean carbon sequestration. *AIChE J*. 2003;49:283–285.
12. Lee SY, Liang L, Rienstenberg DE, West OR, Tsouris C, Adams EE. CO_2 hydrate composite for ocean carbon sequestration. *Environ Sci Technol*. 2003;37:3701–3708.
13. Riestenberg D, Riestenberg D, Chiu E, Gborigi M, Liang L, West OR, Tsouris C. Investigation of jet breakup and droplet size distribution of liquid CO_2 and water systems—implications for CO_2 hydrate formation for ocean carbon sequestration. *Am Mineral*. 2004;89:1240–1246.
14. Riestenberg D, Tsouris C, Brewer P, Peltzer E, Walz P, Chow A, Adams EE. Field studies on the formation of sinking CO_2 particles for ocean carbon sequestration: effects of injector geometry on particle density and dissolution rate and model simulation of plume behavior. *Environ Sci Technol*. 2005;39:7287–7293.
15. Tsouris C, Szymcek P, Taboada-Serrano P, McCallum SD, Brewer P, Peltzer E, Walz P, Adams E, Chow A, Johnson WK, Summers J. Scaled-up ocean injection of CO_2-hydrate composite particles. *Energy Fuels*. 2007;21:3300–3309.
16. Tsouris C, McCallum S, Aaron D, Riestenberg D, Gabitto J, Chow A, Adams E. Scale-up of a continuous-jet hydrate reactor for CO_2 ocean sequestration. *AIChE J*. 2007;53:1017–1027.
17. Szymcek P, McCallum SD, Taboada-Serrano P, Tsouris C. A pilot-scale continuous-jet hydrate reactor. *Chem Eng J*. 2008;135:71–77.
18. Tajima H, Yamasaki A, Kiyono F, Teng H. A new method for ocean disposal of CO_2 via a submerged Kenics-type static mixer. *AIChE J*. 2004;50:871–878.
19. Tajima H, Yamasaki A, Kiyono F. Process design of a new injection process of liquid CO_2 in the ocean by using a static mixer—prediction of the fate of the released liquid CO_2 drop in the ocean and energy dissipation of the process. *Fuel Proc Technol*. 2005;86:1667–1678.
20. Tajima H, Yamasaki A, Kiyono F, Teng H. Size distribution of CO_2 drops in water in a static mixer for ocean disposal. *AIChE J*. 2006;52:2991–2996.
21. Middleman S. Drop size distributions produced by turbulent pipe flow of immiscible fluids through a static mixer. *Ind Eng Chem Process Des Dev*. 1974;13:78–83.
22. Taweel AM, Walker LD. Liquid dispersion in static in-line mixers. *Can J Chem Eng*. 1983;61:527–533.
23. Berkman PD, Calabrese RV. Dispersion of viscous liquids by turbulent flow in a static mixer. *AIChE J*. 1988;34:602–609.
24. Crowe C, Sommerfeld M, Tsuji Y. *Multiphase Flows with Droplets and Particles*. Boca Raton: CRC Press, 1998.
25. Pahl MH, Muschelknautz E. Static mixers and their applications. *Int Chem Eng*. 1982;22:197–205.
26. Hobbs DM, Muzzio FJ. Effects of injection location, flow ratio and geometry on Kenics mixer performance. *AIChE J*. 1997;43:3121–3132.
27. Leng DE, Calabrese RV. *Immiscible liquid–liquid systems*. In: Paul L, Atiemo-Obeng VA, Kresta SM, editors. *Handbook of Industrial Mixing—Science and Practice*. Hoboken: Wiley, 2004:639–754.
28. Wieringa J, Kieft V. Emulsification with static mixer. *Chem Ing Tech*. 1996;68:1137.

29. Uchida T, Kawabata J. Measurements of mechanical properties of the liquid CO_2-Water-CO_2-hydrate system. *Energy*. 1997;22:357–361.
30. Etchells AW III, Meyer CF. *Mixing in pipelines*. In: Paul L, Atiemo-Obeng VA, Kresta SM, editors. *Handbook of Industrial Mixing—Science and Practice*. Hoboken: Wiley, 2004:391–477.
31. Bird RB, Stewart WE, Lightfoot EN. *Transport Phenomena*, 2nd revised ed. New York: Wiley, 2006.
32. Song HS, Han SP. A general correlation for pressure drop in a Kenics static mixer. *Chem Eng Sci*. 2005;60:5696–5704.
33. Grace HP. Dispersion phenomena in high viscosity immiscible fluid systems and application of static mixers as dispersion devices in such systems. *Chem Eng Commun*. 1982;14:225–277.

Manuscript received Jun. 12, 2009, revision received Oct. 13, 2009, and final revision received Dec. 11, 2009.